Journal of Molecular Catalysis A: Chemical 355 (2012) 61–68

Contents lists available at SciVerse ScienceDirect

Journal of Molecular Catalysis A: Chemical

journal homepage: www.elsevier.com/locate/molcata

Review

Mechanism of —O—O— bond activation and substrate oxidation by Ru-edta complexes

Debabrata Chatterjee[a,*], Rudi van Eldik[b]

[a] Chemistry and Biomimetics Group, Central Mechanical Engineering Research Institute, M.G. Avenue, Durgapur 713209, India
[b] Department of Chemistry and Pharmacy, University of Erlangen-Nürnberg, Egerlandstrasse 1, 91058 Erlangen, Germany

ARTICLE INFO

Article history:
Received 26 September 2011
Accepted 11 December 2011
Available online 22 December 2011

Keywords:
Ru-edta complex
Kinetics
Catalysis
—O—O— bond activation
Reaction mechanism
Oxidation of organic substrates

ABSTRACT

This paper presents a short review related to the chemistry of Ru-edta complexes that exhibit catalytic properties in the presence of oxygen atom donors under homogeneous conditions that mimic biological enzymatic hydrocarbon oxidation by cytochrome P450. The results of our recently published work are reviewed in this paper. The mechanism of the reaction of $[Ru^{III}(edta)(H_2O)]^-$ with different oxygen atom donors leading to the formation of various catalytic active species, viz. $[Ru^{III}(edta)(OOH)]^{2-}$, $[Ru^{IV}(edta)(OH)]^-$ and $[Ru^{V}(edta)(O)]^-$, along with their spectral characteristics, are analyzed. Details of the reaction mechanisms have been revealed for peroxide, —O—O— bond activation involving the Ru-edta complex. Furthermore, various mechanistic aspects of the oxidation of organic substrate catalyzed by the Ru-edta complexes are also covered in this report.

Contents

1. Introduction

Ru-edta complexes have been extensively studied over the years because they enjoy a combination of unique properties: (a) the number of stable and accessible oxidation states they posses and (b) high lability towards aqua substitution reactions that affords a straight forward synthesis of mixed ligand complexes that has allowed to explore a wide variety of areas including catalysis [1] and bioinorganic applications [2]. The donor character of the 'edta' ligand is comparable with that of many biological enzymes which make use of carboxylate and amine donors from amino acids to bind to the ruthenium center to form a stable 1:1 (metal:ligand) complex as shown in Fig. 1. The sixth coordination site of the Ru^{III}(edta) complex is occupied either at low pH by a water molecule or at high pH by an hydroxide ion (see Scheme 1). The pK_a values related to the acid-dissociation equilibria of the pendant carboxylic acid arm and the coordinated water molecule are 2.4 and 7.6, respectively, at 25 °C [3,4]. The Ru^{III}(edta) complex predominantly exists in its most labile $[Ru(edta)(H_2O)]^-$ (**1b**) form in the pH range 4.0–6.0 [3,4].

From a catalytic point of view the significance of Ru-edta complexes as oxidation catalysts pertaining to olefin epoxidation and alkane hydroxylation has been reported in the literature [1]. In this article some recent results achieved by the application of fast kinetic techniques to the reactions of $[Ru^{III}(edta)(H_2O)]^-$ with

* Corresponding author. Tel.: +91 343 6510263; fax: +91 343 2546745.
E-mail address: dchat57@hotmail.com (D. Chatterjee).

1381-1169/$ – see front matter © 2012 Elsevier B.V. All rights reserved.
doi:10.1016/j.molcata.2011.12.017

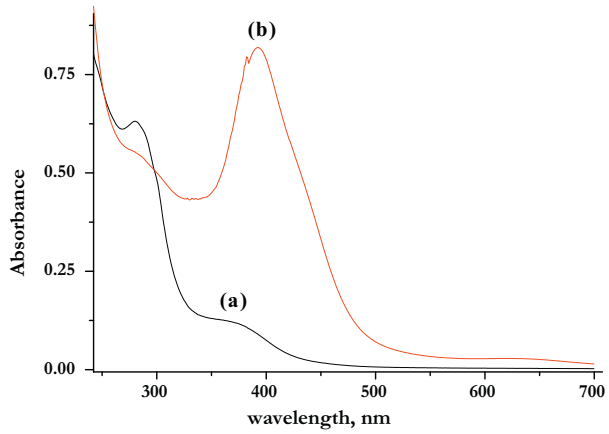

Fig. 1. Spectra of $[Ru^{III}(edta)(H_2O)]^-$ (a) and $[Ru^{V}(edta)(O)]^-$ (b) in water at 25 °C and pH = 5.2.

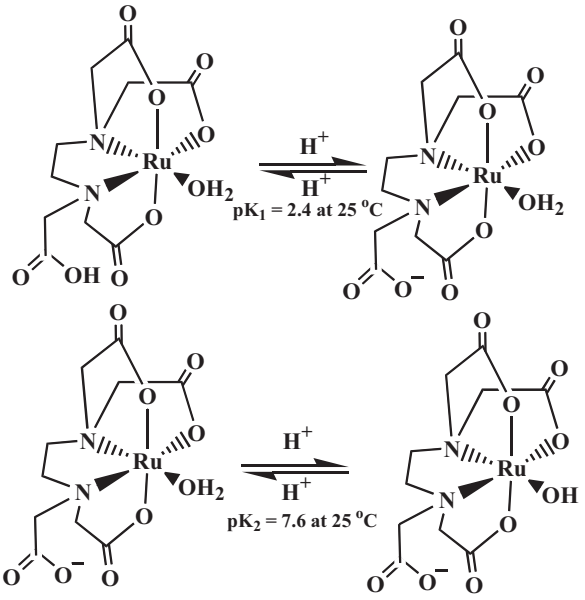

Scheme 1. Proton dissociation equilibria of different Ru^{III}(edta) complexes in aqueous solution.

different oxidants containing an O—O bond that lead to the formation of various catalytically active intermediate species are discussed, and their effectiveness towards the oxidation of some compounds of biological significance are highlighted. The purpose of the present paper is to shed more light on the detailed mechanistic understanding of such important catalytic reactions in inorganic/bioinorganic chemistry.

2. Discussion

The reactivity of the $[Ru^{III}(edta)(H_2O)]^-$ complex towards the activation of several oxygen atom donors, viz. ROOH = H_2O_2, t-BuOOH and HSO_5^-, followed kinetically using stopped-flow and rapid scan spectrophotometric techniques has recently been reported [5,6]. The activation of peroxo bond in ROOH first involves the coordination of ROOH to the Ru(III) center, followed by homolysis or heterolysis of the peroxo O—O bond, which leads to the formation of high-valence ruthenium oxo complexes that are able to transfer oxygen to inert substrate molecules. In the selection of appropriate reaction systems whose mechanisms will be presented below, the liberty of extending this to catalytic reactions is

$$[Ru^{III}(edta)(H_2O)]^- + H_2O_2 \overset{K}{\rightleftharpoons} \{[Ru^{III}(edta)(H_2O)]^-.\ H_2O_2\} \quad (3)$$

$$\{[Ru^{III}(edta)(H_2O)]^-.\ H_2O_2\} \underset{k_{-1}}{\overset{k_1}{\rightleftharpoons}} [Ru^{III}(edta)(OOH)]^{2-} + H_3O^+ \quad (4)$$

$$[Ru^{III}(edta)(OOH)]^{2-} \xrightarrow{k_2} [Ru^{V}(edta)(O)]^- + OH^- \quad (5)$$

$$[Ru^{III}(edta)(OOH)]^{2-} \xrightarrow[H^+]{k_3} [Ru^{IV}(edta)(OH)]^- + OH^\bullet \quad (6)$$

Scheme 2. Proposed reaction scheme for the reaction of $[Ru^{III}(edta)(H_2O)]^-$ with H_2O_2.

exercised. The following sections are in no particular chronological order.

2.1. Reaction of Ru-edta with H_2O_2

The reaction of $[Ru^{III}(edta)(H_2O)]^-$ with H_2O_2 leads to the rapid formation of the hydroperoxo species, $[Ru^{III}(edta)(OOH)]^{2-}$, which subsequently undergoes heterolysis and homolysis of the O—O bond to form $[Ru^{V}(edta)(O)]^-$ and $[Ru^{IV}(edta)(OH)]^-$, respectively (see reactions (3)–(6) in Scheme 2). The $[Ru^{IV}(edta)(OH)]^-$ complex shows no characteristic band in the UV–vis region [7], whereas the $[Ru^{V}(edta)(O)]^-$ complex is characterized by a band at 391 nm ($\varepsilon_{max} = 8000 \pm 20\ M^{-1}\ cm^{-1}$) [8] as shown in Fig. 1, and is the major species formed in solution.

The overall second-order rate constant reported for the formation of $[Ru^{V}(edta)(O)]^-$ was found to be 26.5 $M^{-1}\ s^{-1}$ at 25 °C and pH 5.1 [3]. However, while studying the catalytic degradation [11] of Orange II (a typical azo dye), the reaction of $[Ru^{III}(edta)(H_2O)]^-$ with H_2O_2 was reinvestigated at a higher concentration of H_2O_2 (up to 0.05 M) over the pH range 1–5 using rapid-scan and stopped-flow techniques. Under such conditions rapid formation of a shoulder in the 390 nm band at 425 nm on going to higher H_2O_2 concentrations, followed by a decrease in the intensity of the shoulder accompanied by a further increase in the absorbance at 390 nm, characteristic for the $[Ru^{V}(edta)(O)]^-$ complex, was observed [11]. A typical example of the observed spectral changes at pH 4 is shown in Fig. 2, from which the kinetic trace at 425 nm clearly demonstrates the intermediate nature of the species formed at this wavelength. It should be noted that in most cases the shoulder at 425 nm is formed along with the band at 390 nm and its significance is only controlled by the H_2O_2 concentration and the pH of the solution.

Based on these observations the shoulder at 425 nm was assigned to the formation of the $[Ru^{III}(edta)(OOH)]^{2-}$ complex that subsequently undergoes heterolytic and homolytic cleavage of the peroxo bond to produce $[Ru^{V}(edta)(O)]^-$ and $[Ru^{IV}(edta)(OH)]^-$, respectively. Note that these complexes are the equivalents of Compounds 0, I and II heavily discussed in terms of their role in biomimetic oxidation processes [10,11]. The formation and decay of the $[Ru^{III}(edta)(OOH)]^{2-}$ complex were followed kinetically on a stopped-flow instrument as a function of H_2O_2, and the formation of the $[Ru^{III}(edta)(OOH)]^{2-}$ complex exhibited saturation kinetics revealed at high $[H_2O_2]$, whereas the subsequent decay of the $[Ru^{III}(edta)(OOH)]^{2-}$ complex was found to be independent of the $[H_2O_2]$. The saturation kinetics at very high $[H_2O_2]$ can be accounted for in terms of the rapid formation of a precursor complex, $\{[Ru^{III}(edta)(H_2O)]^-{\cdot}H_2O_2\}$, in the reaction between $[Ru^{III}(edta)(H_2O)]^-$ and H_2O_2 as proposed in the above postulated mechanism (Scheme 2).

The values of K, k_1, and k_{-1} were reported to be $51 \pm 8\ M^{-1}$, $0.86 \pm 0.06\ s^{-1}$ and $0.04 \pm 0.01\ s^{-1}$, respectively [11]. The overall equilibrium constant K_1 ($=Kk_1/k_{-1}$) then has the value $1100 \pm 270\ M^{-1}$, which is in good agreement with an independently determined value for K_1 [11]. The product $K_1(k_2 + k_3)$ presents the

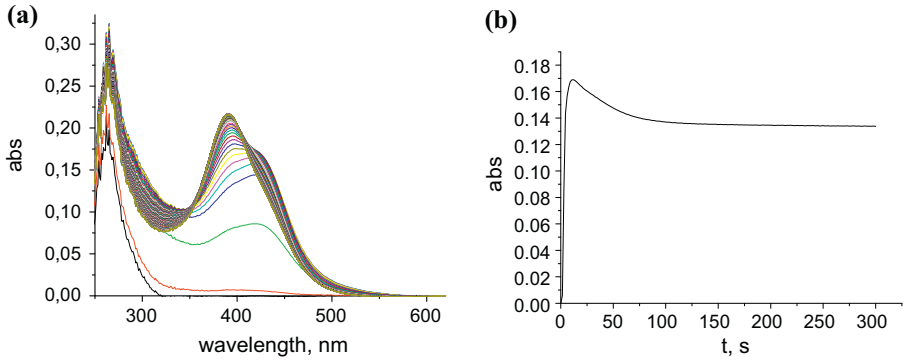

Fig. 2. (a) Spectral changes observed for the reaction of $[Ru^{III}(edta)(H_2O)]^-$ with a high excess of H_2O_2. (b) Absorbance versus time trace at 425 nm. Experimental conditions: $[Ru^{III}] = 4 \times 10^{-5}$ M, $[H_2O_2] = 1 \times 10^{-2}$ M, pH = 4.0 (1 mM acetate buffer), temp. 22 °C.

second-order rate constant for the formation of $[Ru^{IV}(edta)(OH)]^-$ and $[Ru^{V}(edta)(O)]^-$ and has a value of $33 \pm 8\ M^{-1}\ s^{-1}$ at pH 3 and 25 °C based on the equilibrium and rate constants given above ($k_2 = 22 \pm 1\ M^{-1}\ s^{-1}$ and $k_3 = 153 \pm 7\ M^{-1}\ s^{-1}$). This value is close to the value of $26.5\ M^{-1}\ s^{-1}$ found in our earlier study [3] for the direct formation of $[Ru^{IV}(edta)(OH)]^-$ and $[Ru^{V}(edta)(O)]^-$ at pH 5.1 (0.1 M acetate buffer) and 25 °C.

2.2. Reaction of Ru-edta with t-BuOOH and $KHSO_5$

The kinetic behavior of the reaction of $[Ru^{III}(edta)(H_2O)]^-$ with ROOH = ^{t}BuOOH and $KHSO_5$ [4] was found to be similar to that observed for the reaction of $[Ru^{III}(edta)(H_2O)]^-$ with H_2O_2 [3,11]. Similar UV–vis spectral changes with time was noticed (Fig. 3a) for the reaction of $[Ru^{III}(edta)(H_2O)]^-$ with ROOH [4] upon mixing aqueous solutions of $[Ru^{III}(edta)(H_2O)]^-$ and ROOH in the chamber of the stopped-flow instrument equipped with a rapid scan spectral attachment. Spectral changes with time for the reaction of $[Ru^{III}(edta)(H_2O)]^-$ with ^{t}BuOOH shown in Fig. 3a were analyzed with SPECFIT. The SVD (Singular Value Decomposition) analysis of the spectral data in Fig. 3a showed the presence of an intermediate, assumed to be $[Ru^{III}(edta)(OOR)]^{2-}$. The predicted concentration–time profiles from a typical global fit analysis are shown in Fig. 3b.

The reaction was found to consist of two steps involving the rapid formation of a $[Ru^{III}(edta)(OOR)]^{2-}$ intermediate, which subsequently undergoes heterolytic cleavage to form $[Ru^{V}(edta)(O)]^-$. Since $[Ru^{V}(edta)(O)]^-$ was produced almost quantitatively in the reaction of $[Ru^{III}(edta)(H_2O)]^-$ with the hydroperoxides ^{t}BuOOH and $KHSO_5$ [4], the common mechanism is one of heterolytic scission of the O—O bond. The values of the overall second-order rate constants, expressed as kK, i.e. the product of the equilibrium constant K for the formation of $[Ru^{III}(edta)(OOR)]^{2-}$ (R = ^{t}Bu and SO_3^-) and the rate constant k for the subsequent heterolytic cleavage of the O—O bond to form $[Ru^{V}(edta)(O)]^-$, are 1.45 and $7.0\ M^{-1}\ s^{-1}$ for ^{t}BuOOH and $KHSO_5$, respectively, at 25 °C [4]. Since the overall reaction is a two step process as typically outlined in Scheme 2, the ability to form $[Ru^{III}(edta)(OOR)]$ (R = H, ^{t}Bu and HSO_3^-) will partially govern the efficiency of the precursor oxidants (ROOH) to form $[Ru^{V}(edta)(O)]^-$ as the reactive oxidizing species in solution. Based on the pK_a values of the ROOH oxidants, the basicity of the ROOH species is expected to follow the order $HSO_5^- < H_2O_2 <$ ^{t}BuOOH, which should also be reflected in the equilibrium constant K for the formation of the $[Ru^{III}(edta)(OOR)]$ intermediates. However, according to the experimental observations, K is much larger for H_2O_2 [3,11] and $KHSO_5$ than for ^{t}BuOOH [4], which indicates that the basicity of the ROOH species seems to be less important than the steric hindrance caused by the ^{t}butyl group attached to the hydroperoxide fragment. On the other hand, the formation of $[Ru^{V}(edta)(O)]^-$ from $[Ru^{III}(edta)(OOR)]^{2-}$ will depend on the ability of this complex to undergo heterolytic cleavage of the O—O bond expressed by the rate constant k, which in turn should correlate with the reduction potential of the different hydroperoxides under consideration, i.e. ^{t}BuOOH ($E^0 = 1.15$ V) [12] $\ll H_2O_2$ ($E^0 = 1.78$ V) $\leq HSO_5^-$ ($E^0 = 1.82$ V) [13]. From a combination of the separate trends expected for k and K, and a comparison of the trend observed in the values of kK at 25 °C, it follows that in addition to the electronic factors considered here, steric hindrance

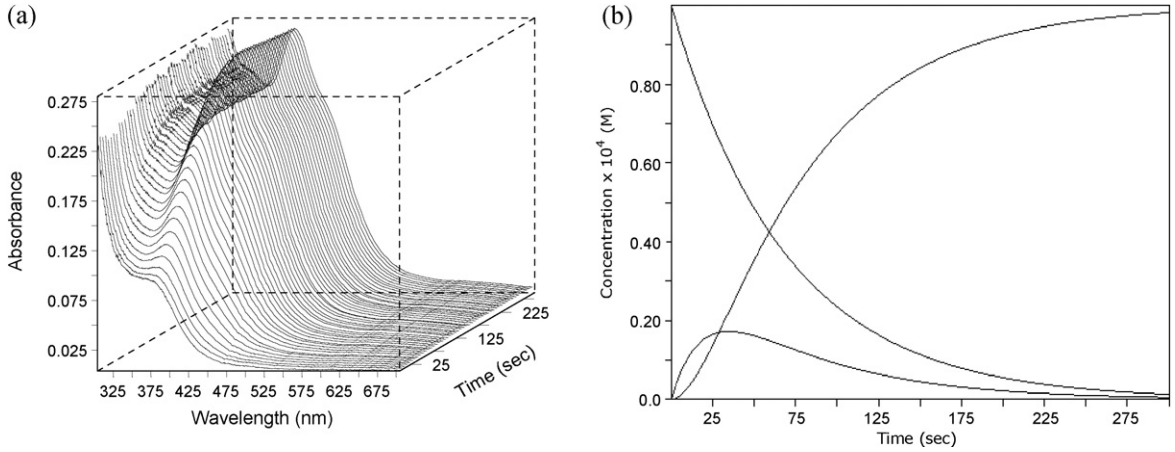

Fig. 3. (a) Spectral changes that occur during the reaction of $[Ru^{III}(edta)H_2O]^-$ (1.0×10^{-4} M) with t-BuOOH (2.5×10^{-3} M) in water at 25 °C and pH = 6.2 (0.2 M acetate buffer). (b) Spectra calculated by the global analysis software package (SPECFIT) for the reaction between $[Ru^{III}(edta)H_2O]^-$ and ^{t}BuOOH.

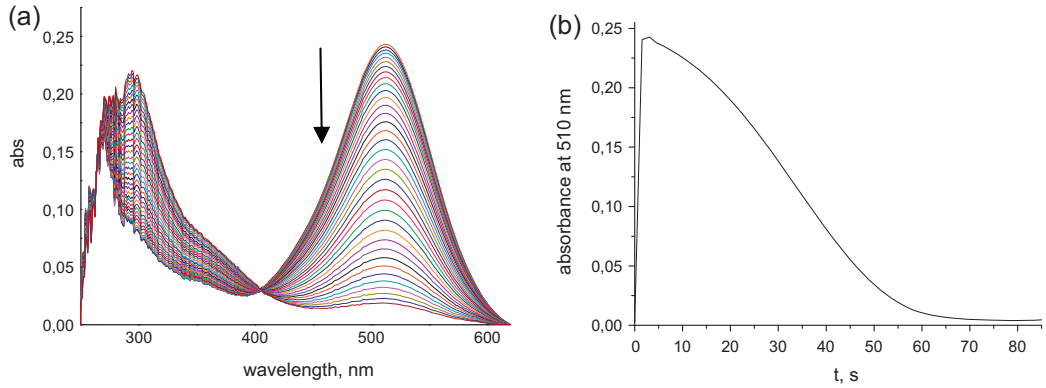

Fig. 4. Spectral changes observed during the reaction of $[Ru^{III}(edta)(SR)]^{2-}$ with H_2O_2. (a) Initial rapid decrease in absorbance at 510 nm. (b) Absorbance versus time plot at 510 nm.

on ^tBuOOH and HSO_5^- as compared to H_2O_2 should further account for the fact that *kK* is significantly smaller for ^tBuOOH and HSO_5^- as compared to H_2O_2. The findings of this work taken together with those for the reaction of $[Ru^{III}(edta)(H_2O)]$ with H_2O_2, strongly suggests that the oxo-transfer from the precursor oxidant ROOH (H_2O_2, ^tBuOOH and $KHSO_5$) to $[Ru^{III}(edta)(H_2O)]$ that results in the formation of the catalytically active $[Ru^{V}(edta)(O)]$ species should proceed through the formation of $[Ru^{III}(edta)(OOR)]^{2-}$ intermediates (R = H, ^tBu and SO_3^-) in a rapid pre-equilibrium step, which subsequently undergoes rate-controlling heterolytic cleavage of the O-O bond to produce $[Ru^{V}(edta)(O)]^-$ as the major product (80–90%). However, in the case of $[Ru^{III}(edta)(OOH)]^{2-}$ formed in the reaction of $[Ru^{III}(edta)(H_2O)]$ with H_2O_2, the subsequent reaction involves both parallel heterolytic and homolytic cleavage to produce $[Ru^{V}(edta)(O)]^-$ and $[Ru^{IV}(edta)(OH)]^-$ in the ratio of approximately 1:1. Thus, the ^tBu and SO_3^- substituents in $[Ru^{III}(edta)(OOR)]^{2-}$ cause O—O bond cleavage to clearly favor heterolysis above homolysis. The results of the reported studies demonstrate the capability to tune the fundamental nature of the O—O bond cleavage process, and underline the advantage of studying such ruthenium-polyaminecarboxylate systems in such detail as reported in this work.

2.3. Oxidation of biologically significant compounds with H_2O_2 catalyzed by Ru-edta complexes

The mechanistic information described above suggests that Ru-edta complexes could be promising species with regard to potential biological applications, especially in the elucidation of the mechanisms of reactive intermediates formed in enzymatic oxygenation reactions that could afford to understand the chemistry of in vivo processes in biological and bioinorganic chemistry.

2.3.1. Oxidation of cysteine with H_2O_2 catalyzed by the Ru-edta complex

Cysteine oxidation with cellular hydrogen peroxide per se is of biological significance with respect to oxidative stress and degenerative neurological disorder [14,15]. Moreover, hydrogen peroxide has been shown to act as a key substance in various intracellular signaling pathways that modulate protein phosphorylation through cysteine oxidation [16]. Recently, the possible role of $[Ru^{III}(edta)(H_2O)]^-$ in protein tyrosine phosphatase (PTP) inhibition of its biological activity was reported [17]. A possible catalytic pathway for the inhibition of PTP by $Ru^{III}(edta)$ in the presence of intracellular H_2O_2 through catalytic oxidation of the cysteine residue was proposed therein [17].

In general, the reaction of $[Ru^{III}(edta)(H_2O)]^-$ with thiols leads to the formation of characteristically colored, S-coordinated $[Ru^{III}(edta)SR]^{2-}$ complexes [18]. $[Ru^{III}(edta)(H_2O)]^-$ reacts rapidly with cysteine (RSH) to form the red colored $[Ru^{III}(edta)(SR)]^{2-}$ complex (λ_{max} = 510 nm, ε_{max} = 3330 M^{-1} cm^{-1}) with a complex-formation constant (K_1 in reaction (7)) of 3×10^5 M^{-1} at 25 °C and pH 5 [18]. Addition of an excess of H_2O_2 to the $[Ru^{III}(edta)(SR)]^{2-}$ solution resulted in a rapid decay of the band at 510 nm which is attributed to the oxidation of the coordinated cysteine in $[Ru^{III}(edta)(SR)]^{2-}$ by H_2O_2 under the specified conditions [19]. When the experiment is carried out under the condition $[Ru^{III}]$:[RSH]:$[H_2O_2]$ = 1:1:1, only the decay of the band at 510 nm is observed and the final spectrum is in full agreement with that for the $[Ru^{III}(edta)(H_2O)]^-$ complex (Fig. 4). Addition of cysteine to the latter solution rapidly leads to the reformation of $[Ru^{III}(edta)(SR)]^{2-}$.

The observed reactions under turn-over conditions, e.g. $[Ru^{III}]$:[RSH]:$[H_2O_2]$ = 1:10:100, can be accounted for in terms of the suggested reaction mechanism outlined in reactions (7)–(12), which is based on detailed kinetic experiments, product analyses and simulations of the observed kinetic traces, described in more detail below [11].

In the proposed reaction scheme, reactions (7) and (8) are responsible for the oxidation of coordinated cysteine to RSOH (cysteine sulfenic acid), for which reaction (8) is the rate-determining step. Similar reactions were found to occur for the reaction of H_2O_2 with thiolato complexes of Cr(III) [20]. Subsequently, $[Ru^{III}(edta)(SROH)]^-$ reacts rapidly with H_2O_2 and RSH in reactions (9) and (10) to form RSO_2H (cysteine sulfenic acid) and RSSR (cystine), respectively. Evidence for the oxidation products formed in reactions (9) and (10) came from HPLC analyses. Both reactions (9) and (10) simultaneously regenerate $[Ru^{III}(edta)H_2O]^-$ that in turn rapidly coordinates free cysteine to mediate its further oxidation via reactions (7) and (8). The formation of RSOH has been reported in the literature [21,22] and can undergo a rapid subsequent reaction with RSH to produce RSSR (cystine) [23]. In the absence of $[Ru^{III}(edta)(H_2O)]^-$, RSH is only partially oxidized even after 900 s to form mainly RSSR along with trace amounts of RSO_2H as evidenced from HPLC analysis. These results convincingly demonstrate the catalytic role of $[Ru^{III}(edta)(H_2O)]^-$ in the oxidation of RSH by H_2O_2. The product distribution as a function of [RSH] further suggested that reaction (10) must be significantly faster than reaction (9), and an average value for k_4/k_3 of ca. 8 could be calculated. In all cases, complete consumption of cysteine was observed.

Since the $[Ru^{V}(edta)O]^-$ species is known to affect the oxidation of organic substrates [1], the reaction of $[Ru^{V}(edta)O]^-$ with cysteine via reaction (12) was also examined, and the values of the observed first-order rate constants were found to increase linear with increasing [cysteine], which resulted in a k_6 value of

$$[Ru^{III}(edta)(H_2O)]^- + RSH \underset{k_{-1}}{\overset{k_1}{\rightleftharpoons}} [Ru^{III}(edta)(SR)]^{2-} + H_3O^+ \quad K_1 = k_1/k_{-1} \qquad (7)$$

$$[Ru^{III}(edta)(SR)]^{2-} + H_2O_2 \xrightarrow{k_2} [Ru^{III}(edta)(SROH)]^- + OH^- \qquad (8)$$

$$[Ru^{III}(edta)(SROH)]^- + H_2O_2 \xrightarrow{k_3} [Ru^{III}(edta)(H_2O)]^- + RSO_2H \qquad (9)$$

$$[Ru^{III}(edta)(SROH)]^- + RSH \xrightarrow{k_4} [Ru^{III}(edta)(H_2O)]^- + RSSR \qquad (10)$$

$$[Ru^{III}(edta)(H_2O)]^- + H_2O_2 \xrightarrow{k_5} [Ru^{V}(edta)O]^- + 2H_2O \qquad (11)$$

$$[Ru^{V}(edta)O]^- + RSH \xrightarrow{k_6} [Ru^{III}(edta)(SROH)]^- \qquad (12)$$

Scheme 3. Mechanistic scheme for the Ru-edta catalyzed oxidation of RSH with H_2O_2.

$(8.9 \pm 0.7) \times 10^{-2}\ M^{-1}\ s^{-1}$ at 20 °C. It follows that the values of k_5 and k_6 are much smaller than those of k_1 and k_2, which accounts for the fact that reactions (11) and (12) cannot compete with reactions (7) and (8) as long as there is free cysteine in the solution. Thus $[Ru^{III}(edta)(H_2O)]^-$ can effectively mediate the oxidation of cysteine by rapidly binding cysteine prior to the reaction with H_2O_2.

The complex nature of the kinetic trace as typically shown in Fig. 4b indicate the involvement of different reaction steps as outlined by reactions (7)–(12) given in Scheme 3. In order to further substantiate the mechanism proposed in Scheme 3, simulation studies were performed using SPECFIT, Global Analysis System, Version 3.0.37 for 32-bit Windows system and Pro-Kinetic Analysis, Version 1.08. In fact, at this stage of the investigation it was unknown what actually happened kinetically to the cysteine sulfenic acid formed in reaction (2). Some typical absorbance–time traces as a function of H_2O_2, along with the simulated traces based on the reaction sequence outlined in reactions (7)–(12), are presented in Fig. 5.

The simulated absorbance–time traces shown in Fig. 5 are in close agreement with the experimental ones. A comparison of the experimental and simulated rate constants in Table 1 show a rather close agreement for the rate constants k_1, k_{-1}, k_2 and k_5. The

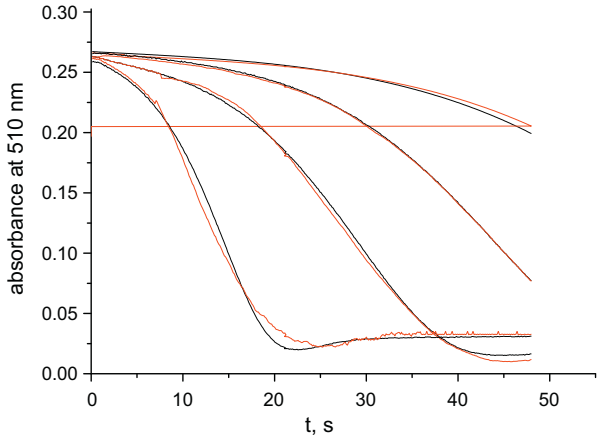

Fig. 5. Experimental (black) and simulated (red) absorbance–time traces at 510 nm for the reaction of $[Ru^{III}(edta)(SR)]^{2-}$ (preformed by reacting $[Ru^{III}(edta)(H_2O)]^-$ with cysteine in the ratio 1:1) with different concentrations of H_2O_2. Experimental conditions: $[Ru^{III}] = 1 \times 10^{-4}$ M, [cysteine] = 1×10^{-4} M, $[H_2O_2] = (1, 2, 3$ and $6) \times 10^{-3}$ M (increasing from right to left), pH 5.1, temp. 20 °C. (For interpretation of the references to color in this figure legend, the reader is referred to the web version of this article.)

Table 1
Summary of experimental and simulated rate constants data determined at 20 °C.

Rate constant	Experimental value	Simulated value
k_1	$170 \pm 6\ M^{-1}\ s^{-1}$	$177 \pm 13\ M^{-1}\ s^{-1}$
k_{-1}	$(5.7 \pm 0.3) \times 10^{-4}\ s^{-1}$	$(5 \pm 1) \times 10^{-4}\ s^{-1}$
k_2	$22 \pm 1\ M^{-1}\ s^{-1}$	$21.6 \pm 1.1\ M^{-1}\ s^{-1}$
k_3	–	$153 \pm 7\ M^{-1}\ s^{-1}$
k_4	–	$928 \pm 64\ M^{-1}\ s^{-1}$
k_5	$15.4 \pm 0.6\ M^{-1}\ s^{-1}$	$15.8 \pm 0.6\ M^{-1}\ s^{-1}$
k_6	$0.089 \pm 0.007\ M^{-1}\ s^{-1}$	$0.83 \pm 0.07\ M^{-1}\ s^{-1}$

simulated value of k_6 is an order of magnitude larger than the experimental value, which is presumably related to the fact that reaction (12) is indeed very slow and hardly contributes to the overall process under the selected reaction conditions, making its estimation rather inaccurate on the time scale of the studied reactions.

Interestingly, the simulated rate constant k_4 for reaction (10) is high, ca. 6 times larger than k_3 for reaction (9), which is in close agreement with the predicted ratio of k_4/k_3 (ca. 8) based on the chromatographic analyses performed as a function of RSH concentration. The values of k_2 and k_4 are also quite remarkable in that their values and ratio agree quite closely with the rate constants reported for the spontaneous reactions (13) and (14), respectively [23]. The reaction of RSOH with RSH leading to the formation of RSSR is much faster than the reaction of RSOH with H_2O_2 (which results in formation of RSO_2H), because RSSR was found to be the major oxidation product in the oxidation of RSH with H_2O_2 [23].

$$RS^- + H_2O_2 \rightarrow RSOH + OH^- \qquad k = 15\ M^{-1}\ s^{-1} \qquad (13)$$

$$RSOH + RS^- \rightarrow RSSR + OH^- \qquad k = 720\ M^{-1}\ s^{-1} \qquad (14)$$

This close agreement suggests that the role of $Ru^{III}(edta)$ in the complex-mediated reactions (8) and (10) is similar to that caused by an increase in pH from 5 to 10 to deprotonate RSH for the spontaneous reactions. Thus, coordination of RSH and RSOH to $Ru^{III}(edta)$ increases the oxidation reactivity of these species in the same way as deprotonation of one of the reaction partners caused by a drastic increase in pH. This is surely related to the Lewis acidity of the $Ru^{III}(edta)$ center. The S-bonded $[Ru^{III}(edta)(SROH)]^-$ intermediate species is formed via the oxidation of coordinated thiol in $[Ru^{III}(edta)(SR)]^{2-}$. This intermediate is vulnerable towards attack of H_2O_2 under the specified conditions leading to the formation of RSO_2H (identified and quantified by HPLC analysis).

All in all, the performed simulations show a satisfactory agreement with the experimental kinetic traces and data, and support the validity of the suggested reaction mechanism, which can be

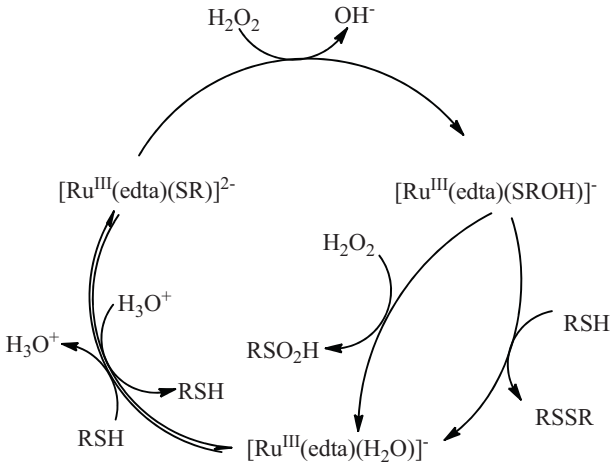

Scheme 4. Overall catalytic cycle showing how $[Ru(edta)(H_2O)]^-$ mediates the oxidation of cysteine by H_2O_2 in a weakly acidic aqueous solution.

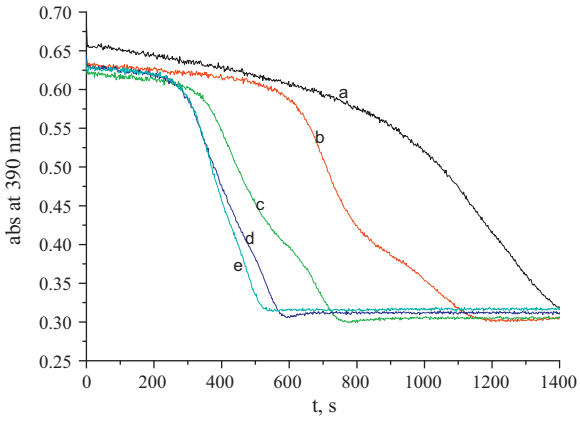

Fig. 6. Absorbance vs. time trace at 390 nm for the of $[Ru^{III}(edta)(H_2O)]^-$ mediated oxidation of HOU by H_2O_2 at pH 5.0, 25 °C, $[Ru^{III}] = 1.0 \times 10^{-4}$ M, $[H_2O_2] = 1.0 \times 10^{-4}$ M and $[HOU] = 1 \times 10^{-3}$ (a), 2×10^{-3} (b), 4×10^{-3} (c), 5×10^{-3} (d) and 6×10^{-3} M (e).

summarized schematically as shown in Scheme 3. The parallel reactions (11) and (12) that involve the formation of $[Ru^V(edta)O]^-$ as catalyst cannot compete with the efficiency of this catalytic cycle.

The Ru^{III}-edta complex capable of mediating the oxidation of cysteine using H_2O_2 as oxidant under ambient conditions thus mimicking the action of cysteine peroxidase has special relevance to biological systems, since it has been recognized that hydrogen peroxide can act as a key messenger in different intracellular signaling pathways that modulate the action of a group of enzymes, viz. phosphatases and kinases, through oxidation of cysteine residues (Scheme 4).

2.3.2. Oxidation of N-hydroxyurea with H_2O_2 catalyzed by the Ru-edta complex

Oxidation of hydroxyurea is of special significance with regard to its therapeutic use in the treatment of sickle cell diseases [24,25]. It was reported earlier that the oxidation of hydroxyurea (HOU) by H_2O_2 alone is slow [26]. However, horseradish peroxydase (HRP) [27] and catalase [28] catalyze the oxidation of hydroxyurea (Scheme 5).

Some recent reports [29,30] suggest that hydroxyurea may mediate some of its effect via nitric oxide (NO) production. As a matter of fact sickle cell patients demonstrate in vivo NO formation during HOU therapy [29,31]. In a recent paper the ability of $[Ru^{III}(edta)(H_2O)]^-$ to oxidize HOU in resemblance with enzymatic oxidation of HOU has been demonstrated [32], and the results reported are of significance to provide further mechanistic insight as the detailed molecular mechanism of HOU oxidation remains unsettled. Spectral measurements of the time course of the oxidation of HOU exhibited typical zero-order kinetic traces following the induction period (see Fig. 6) recorded at 390 nm for the depletion of the high-valence $[Ru^V(edta)(O)]^-$ species in the reaction system.

The reported kinetic observations together with an apparent induction period is consistent with a mechanism (Scheme 6) in which the reaction is initiated by $[Ru^{IV}(edta)(OH)]^-$ species formed in the reaction of the complex $[Ru^{III}(edta)(H_2O)]^-$ with H_2O_2. The rate-determining step of the process is outlined in part B where $[Ru^{IV}(edta)(OH)]^-$ reacts with HOU to form the hydroxyurea radical and $[Ru^{III}(edta)(H_2O)]^-$. Subsequently, the hydroxyurea radical rapidly reacts with $[Ru^V(edta)(O)]^-$ to reproduce $[Ru^{IV}(edta)(OH)]^-$ in part C of Scheme 6. In this way the concentration of $[Ru^{IV}(edta)(OH)]^-$ species (colorless) remains constant throughout the oxidation process for which depletion of $[Ru^V(edta)(O)]^-$ species then exhibits pseudo-zero-order kinetics. The apparent induction period observed in each case (Fig. 6) can be ascribed to the initial formation of $[Ru^V(edta)(O)]^-$ and $[Ru^{IV}(edta)(OH)]^-$ (part A) and the production of hydroxyurea radicals (part B in Scheme 6). The decrease in the observed induction period with increasing HOU concentration (Fig. 6) implicates an enhancement of the rate of formation of hydroxyurea radicals at higher HOU concentrations in part B of Scheme 6.

Ion-chromatographic analysis of the resulting mixture at the end of the reaction confirmed the formation of nitrite and nitrate in the reaction system. These results are indicative of NO production during the oxidation of hydroxyurea in the presence of hydrogen peroxide. Measurements with a NO sensitive electrode indeed confirmed the release of free NO from HOU, though admittedly at a low concentration level (maximum NO concentration amounted to less than 1.0% of that expected for quantitative liberation from HOU) in the catalyzed oxidation of HOU with H_2O_2. However, it should be noted that we could for the first time provide direct

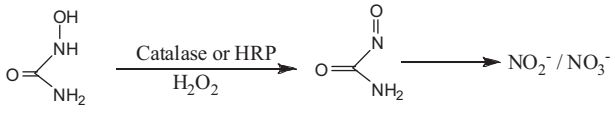

Scheme 5. Oxidation of HOU with H_2O_2 catalyzed by catalase or HRP.

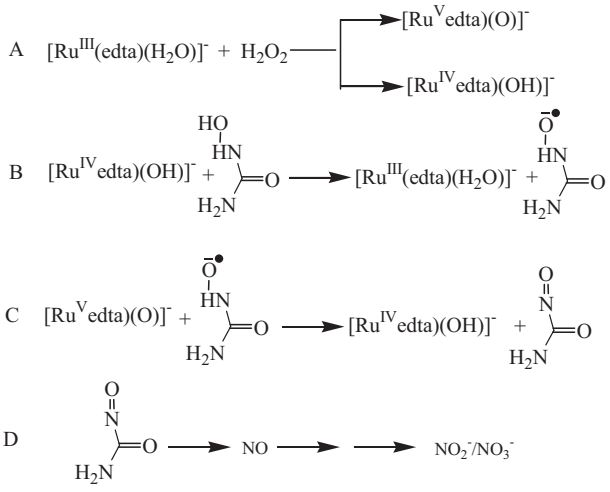

Scheme 6. Mechanism of oxidation of HOU with H_2O_2 catalyzed by Ru-edta complex.

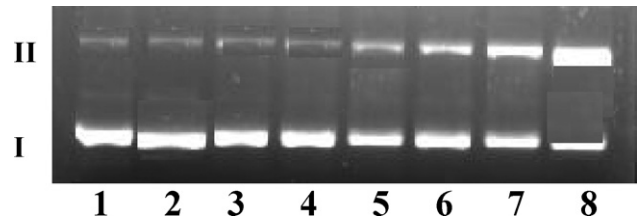

Fig. 7. Cleavage of supercoiled pBluescript (SK^+) plasmid DNA by the Ru-edta complex in Tris–HCl buffer in the presence of ROOH in TAE buffer at 37 °C. Lane 1: the plasmid preparation was good: forms I, II are present, max is form I. Lane 2: $KHSO_5$ (0.5 mM) caused slight DNA nicking, increase in form II. Lane 3: H_2O_2 (0.5 mM) alone caused no DNA nicking. Lane 4: Ru-edta (100 μM) alone caused no DNA nicking. Lane 5: $KHSO_5$ (0.1 mM) + Ru-edta (250 μM); synergistic action; DNA nicking occurred as more of form II present. Lane 6: $KHSO_5$ (0.5 mM) + Ru-edta (250 μM); increased DNA nicking. Lane 7: H_2O_2 (0.1 mM) + Ru-edta (250 μM); synergistic action; DNA nicking occurred as more of form II present. Lane 8: H_2O_2 (0.5 mM) + Ru-edta (250 μM); increased DNA nicking.

evidence for the liberation of free NO during the oxidation of HOU by H_2O_2. Obviously, under the employed conditions the liberated NO rapidly and efficiently undergoes further oxidation by unreacted $[Ru^V(edta)(O)]^-$ to result in the formation of nitrite and nitrate as final product. The liberation of NO during oxidation of HOU under the specified conditions is of obviously of importance in the understanding its biological activity [32].

2.3.3. Oxidative cleavage of DNA with ROOH catalyzed by the Ru-edta complex

The results of the reported studies [5,6] on the reaction of Ru-edta complexes with ROOH stimulated the development of Ru-edta based agents for oxidative cleavage of DNA. Recently, the DNA cleavage activity of Ru-edta in the presence of the primary oxidant ROOH (H_2O_2, $KHSO_5$) was explored [33].

The DNA cleavage efficiency of Ru^{III}-edta was monitored by observing the conversion of supercoiled (form I) plasmid DNA to the circular nicked form (form II) as shown in Fig. 7. Ru^{III}-edta showed an appreciable conversion of supercoiled pBluescript (SK^+) DNA (SC) to nicked circular DNA (nicked) upon prolonged incubation in the presence of ROOH, and the efficacy of DNA cleavage increased with increasing amount of ROOH. Considering that the oxidation of Ru-edta by ROOH leads to formation of high-valence Ru(V)-oxo species [5,6] which are known to oxidize C—H bonds in saturated hydrocarbons [1], it has been presumed that a mechanism involving the high-valence $[(edta)Ru^V=O]^-$ species is operative for the nuclease activity of anionic the Ru-edta complex on supercoiled DNA in the presence of ROOH [33]. Almost identical cleavage patterns reportedly observed for both Ru-edta/$KHSO_5$ and Ru-edta/H_2O_2 plausibly supports the above mechanistic arguments.

2.4. Oxidation of Orange II with H_2O_2 catalyzed by the Ru-edta complex

Among dyes, reactive azo dyes constitute a significant portion of dye pollutants and probably have the least desirable consequences in terms of the surrounding ecosystem [34]. In a very recent study, remarkable catalytic activity of the $[Ru^{III}(edta)(H_2O)]^-$ complex towards degradation of Orange II (ORII), a model azo dye has been reported [11]. A detailed kinetic and mechanistic study of the degradation of ORII by H_2O_2 in the presence of the $[Ru^{III}(edta)(H_2O)]^-$ revealed for the first time direct evidence for the hydroperoxo complex $[Ru^{III}(edta)(OOH)]^{2-}$ as the sole catalytic species for the degradation of ORII by hydrogen peroxide in a pH range from 1 to 5. The highest catalytic activity is reportedly reached [11] immediately after the addition of $[Ru(edta)H_2O]^-$ to a mixture of H_2O_2 and ORII during which $[Ru^{III}(edta)(OOH)]^{2-}$ is rapidly formed. This reaction is three orders of magnitude faster than

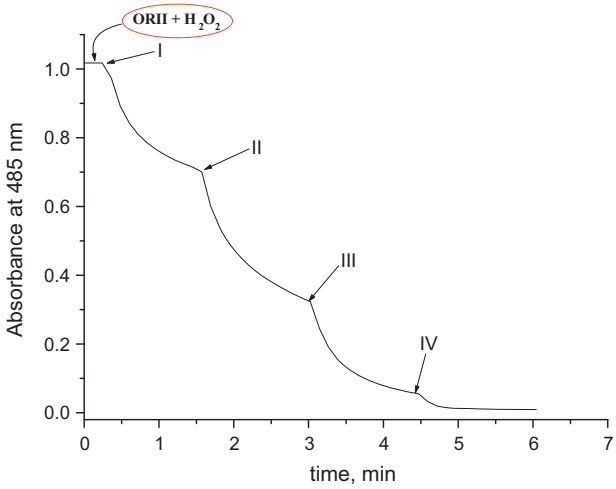

Fig. 8. Degradation of Orange II (5×10^{-5} M) by H_2O_2 (1×10^{-2} M) catalyzed by $[Ru(edta)(H_2O)]^-$ (2×10^{-6} M) at pH = 4.0 (1.0 mM acetate buffer), temp. 20 °C; I–IV indicate the addition of a new aliquot of $[Ru(edta)H_2O]^-$ (2×10^{-6} M).

the reaction of $[Ru^{IV}(edta)(OH)]^-$ and $[Ru^V(edta)(O)]^-$ with ORII. However, if the degradation process is initiated by the addition of ORII after a delay of 500 s, i.e. the time required to produce $[Ru^{IV}(edta)(OH)]^-$ and $[Ru^V(edta)(O)]^-$ from $[Ru(edta)H_2O]^-$ and H_2O_2, the catalytic cycle apparently does not involve the participation of $[Ru^{III}(edta)(OOH)]^{2-}$ anymore. During the turnover of the catalytic cycle there will be a build up of the less active species $[Ru^{IV}(edta)(OH)]^-$ and $[Ru^V(edta)(O)]^-$ since the second order rate constant for the formation of $[Ru^{III}(edta)(OOH)]^{2-}$, viz. $44\pm10\ M^{-1}\ s^{-1}$, is within the error limits, only slightly larger than the rate constant reported for the formation of $[Ru^{IV}(edta)(OH)]^-$ and $[Ru^V(edta)(O)]^-$, viz. $26.5\ M^{-1}\ s^{-1}$ at 25 °C. The consequence of this situation was nicely demonstrated with an experiment where the catalyst was subsequently added in small amounts for which the results are shown in Fig. 8. The traces recorded in Fig. 8 show that at a Ru-edta catalyst concentration of 2×10^{-6} M the initial rapid degradation of ORII ceases after some time and goes over into a very slow reaction. Addition of another portion of the catalyst immediately initiates the degradation again and shows a similar behavior. By the end of the experiment a total of 8×10^{-6} M catalyst was added to the solution during which 5×10^{-5} M of ORII was decomposed. This experiment shows that the concentration of the catalyst is crucial since during the turnover of the cycle more and more of the less active catalytic species $[Ru^{IV}(edta)(OH)]^-$ and $[Ru^V(edta)(O)]^-$ are formed, almost like a dead-end process leading to a much slower catalytic conversion.

In the proposed formation of $[Ru^{III}(edta)(OOH)]^{2-}$ as the intermediate with the highest catalytic activity at pH 4, the role of the dangling acetate arm assisting the intramolecular deprotonation of the coordinated hydrogen peroxide that leads to the stabilization of the hydroperoxo complex $[Ru^{III}(edta)(OOH)]^{2-}$ is schematically demonstrated in Scheme 7. The present study illustrated the remarkably high activity of $[Ru^{III}(edta)(OOH)]^{2-}$, the Ru equivalent of Compound 0, as compared to $[Ru^{IV}(edta)(OH)]^-$ and $[Ru^V(edta)(O)]^-$, the Ru equivalents of Compounds II and I, respectively, towards the degradation of ORII. At much lower pH, protonation of the dangling acetate arm will not allow this intramolecular stabilization of the hydroperoxo intermediate and lead to a decrease in the concentration and catalytic activity of the complex. The dangling acetate ligand is also held responsible for the subsequent homolytic and heterolytic cleavage of the peroxo bond in $[Ru^{III}(edta)(OOH)]^{2-}$.

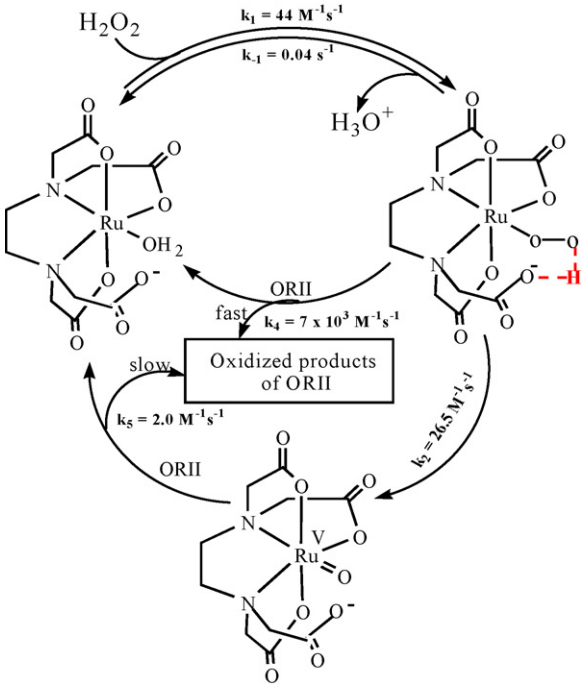

Scheme 7. Proposed catalytic cycle and apparent role of the dangling acetate arm of edta^{4-}.

The $[Ru^{III}(edta)(OOH)]^{2-}$ complex can apparently initiate the degradation of ORII via the cationic pathway suggested for oxygen atom transfer by Compound 0 in P450 type oxidation processes. This rather remarkable finding motivates further detailed studies along the lines of the present report for the biomimetic oxidation of various substrates employing Ru^{III}-edta type compounds. The $[Ru^{III}(edta)(OOH)]^{2-}$ complex demonstrates that the ruthenium equivalent of Compound 0 is many orders more efficient than the equivalent complexes for Compounds I and II, viz. $[Ru^{IV}(edta)(OH)]^{-}$ and $[Ru^{V}(edta)(O)]^{-}$, respectively. This order of reactivity is totally different than recently found for a functional model Fe^{III}(porphyrin) system [9,10] where the equivalent of Compound I showed a much higher catalytic activity for a series of epoxidation, sulfoxidation, O—H abstraction and C—H abstraction reactions, than either the Ru equivalents of Compounds 0 and II.

3. Conclusions

Insight into reaction mechanisms obtained from kinetic studies reported herein should have biological implications. Mechanistically the Ru-edta complex appears to be interesting as the ruthenium equivalent of Compund 0 is much more reactive than that of Compounds I and II. As noted recently [11], whether O—O bond scission precedes substrate activation or occurs through the direct attack of the peroxo unit on the azo bond of ORII is an intriguing unanswered question.

Acknowledgments

This work was also supported by the Department of Science & Technology, Govt. of India, New Delhi (Grant No. SR/S5/BC-15/2006). D.C. is thankful to Prof. Goutam Biswas, Director of the CSIR-CMERI, Durgapur, India for his support of this work. R.v.E. gratefully acknowledges continued financial support from the Deutsche Forschungsgemeinschaft.

References

[1] D. Chatterjee, Coord. Chem. Rev. 16 (1998) 273–293.
[2] D. Chatterjee, A. Mitra, G.S. De, Plat. Met. Rev. 50 (2006) 2–12.
[3] T. Matsubara, C. Creutz, Inorg. Chem. 18 (1979) 1956–1966.
[4] H.C. Bajaj, R. van Eldik, Inorg. Chem. 27 (1988) 4052–4055.
[5] D. Chatterjee, A. Mitra, R. van Eldik, Dalton Trans. (2007) 943–948.
[6] D. Chatterjee, A. Sikdar, V.R. Patnam, A. Theodoridis, R. van Eldik, Dalton Trans. (2008) 3851–3856.
[7] S. Zhang, R.E. Shepherd, Inorg. Chem. 27 (1988) 4712–4719.
[8] M.M. Taqui Khan, D. Chatterjee, R.R. Merchant, P. Paul, S.H.R. Abdi, M.R.H. Siddiqui, D. Srinivas, M.A. Moiz, M.M. Bhadbhade, K. Venkatasubramaniun, Inorg. Chem. 31 (1992) 2711–2718.
[9] A. Franke, C. Fertinger, R. van Eldik, Angew. Chem. Int. Ed. 47 (2008) 5238–5242.
[10] C. Fertinger, N. Hessenauer-Ilicheva, A. Franke, R. van Eldik, Chem. Eur. J. 15 (2009) 13435–13440.
[11] D. Chatterjee, E. Ember, U. Pal, S. Ghosh, R. van Eldik, Dalton Trans. 40 (2011) 10473–10480.
[12] S.Y. Shin, R.E. Marquis, Arch. Microbiol. 161 (1994) 184–190.
[13] J. Balej, J. Electroanal. Chem. 214 (1986) 481–483.
[14] R.A. Floyd, Proc. Exp. Biol. Med. 222 (1999) 236–245.
[15] T. Finkel, N.J. Holbrook, Nature 408 (2000) 239–247.
[16] S.G. Rhee, Science 312 (2006) 1882–1883.
[17] D. Chatterjee, A. Mitra, A. Levina, P.A. Lay, Chem. Commun. (2008) 2864–2866.
[18] (a) D. Chatterjee, M.S.A. Hamza, M.M. Shoukry, A. Mitra, S. Deshmukh, R. van Eldik, Dalton Trans. (2003) 203–209;
(b) V.G. Povse, J.A. Olabe, Trans. Met. Chem. 23 (1998) 657–662;
(c) D. Chatterjee, H.C. Bajaj, J. Coord. Chem. 39 (1996) 117–122.
[19] D. Chatterjee, E. Ember, U. Pal, S. Ghosh, R. van Eldik, Dalton Trans. 40 (2011) 10997–11004.
[20] L.E. Asher, E. Deutsch, Inorg. Chem. 12 (1972) 2927–2933.
[21] M.T. Ashby, P. Nagy, Int. J. Chem. Kinet. 39 (2007) 32–38.
[22] P. Nagy, M.T. Ashby, J. Am. Chem. Soc. 129 (2007) 14082–14091.
[23] D. Luo, W.S. Smith, B.D. Anderson, J. Pharm. Sci. 94 (2005) 304–316.
[24] S. Charache, F.B. Barton, R.D. Moore, M.L. Terrin, M.H. Steinberg, G.J. Dover, S.K. Ballas, P. McMahon, O. Castro, E.P. Orringer, Medicine 75 (1996) 300–326.
[25] M.R. Stevens, J. Biol. Regul. Homeos. Agents 13 (1999) 172–175.
[26] Y. Xu, C.D. Mull, C.L. Bonifant, G. Yasaki, E.C. Palmer, H. Shields, S.K. Ballas, D.B. Kim-Shapiro, S.B. King, J. Org. Chem. 63 (1998) 6452–6453.
[27] J. Huang, D.B. Kim-Shapiro, S.B. King, J. Med. Chem. 47 (2004) 3495–3501.
[28] J. Huang, E.M. Sommers, D.B. Kin-Shapiro, S.B. King, J. Am. Chem. Soc. 124 (2002) 3473–3480.
[29] M. Nahavandi, F. Tavakkoli, M.Q. Wyche, E. Perlin, W.P. Winter, O. Castro, Br. J. Haematol. 119 (2002) 855–857.
[30] V.P. Cokic, R.D. Smith, B.B. Beleslin-Cokic, J.M. Njoroge, J.L. Miller, M.T. Gladwin, A.N. Schechter, J. Clin. Invest. 111 (2003) 231–239.
[31] R.E. Glover, E.D. Ivy, E.P. Orringer, H. Meda, R.P. Mason, Mol. Pharmacol. 55 (1999) 1006–1010.
[32] D. Chatterjee, K.A. Nayak, E. Ember, R. van Eldik, Dalton Trans. 39 (2010) 1695–1698.
[33] D. Chatterjee, C. Hariharan, M. Chatterjee, A. Mitra, J. Coord. Chem. 62 (2009) 1719–1724.
[34] H. Zollinger, Colour Chemistry, Synthesis, Properties and Application of Organic Dyes and Pigments, 3rd ed., Wiley, Weinheim, 2003.